Electrical circuit modeling of conductors with skin effect

D. W. Kerst and J. C. Sprott
University of Wisconsin, Madison, Wisconsin 53706

(Received 19 February 1986; accepted for publication 28 March 1986)

The electrical impedance of a lossy conductor is a complicated function of time (or frequency) because of the skin effect. By solving the diffusion equation for magnetic fields in conductors of several prototypical shapes, the impedance can be calculated as a function of time for a step function of current. The solution suggests an electrical circuit representation that allows calculation of time-dependent voltages and currents of arbitrary waveforms. A technique using an operational amplifier to determine the current in such a conductor by measuring some external voltage is described. Useful analytical approximations to the results are derived.

I. INTRODUCTION

An electrical current flowing in a conductor requires a voltage to sustain both its resistive (IR) and inductive (LdI/dt) components. The resistance is usually calculated in the low-frequency limit where the current density in the conductor has reached its steady-state (often uniform) value. The inductance is usually calculated in the high-frequency limit where the current flows in a thin skin on the surface of the conductor. At intermediate frequencies, the resistance is increased from its dc value by this skin effect, and the inductance is increased from its high-frequency value by the magnetic flux embedded in the conductor. The goal of this paper is to develop methods for predicting the voltage $V(t)$ which results from a current $I(t)$ that has frequency components in this complicated, intermediate regime. A by-product of the calculation is the design of an operational amplifier circuit that allows the time-dependent current in a conductor to be determined by measuring some appropriate voltage. The calculation was motivated by a desire to model toroidal magnetic confinement devices for plasmas surrounded by thick, conducting walls and with internal conducting shells or rings, but the applications extend to any electrical system in which skin effect is important. Skin effect has been calculated for many geometric configurations.[1–5] Modern techniques rely heavily on numerical, finite-element methods.[6–8]

In Sec. II, the one-dimensional diffusion equation for the soak-in of a magnetic field to conductors of various shapes is solved for the special case of a constant magnetic field at the surface of the conductor. For many cases this corresponds to a total current in the conductor that is a step function of time. In Sec. III the results are converted into a time-dependent impedance using the fact that the voltage is the rate at which magnetic flux penetrates the surface of the conductor. In Sec. IV the time-dependent impedance is modeled by an electrical equivalent circuit which allows the results to be generalized to an arbitrary, time-dependent waveform for use in circuit analysis computation codes. In Sec. V an example is given of using the circuit model to represent a coaxial line with a solid resistive center conductor and a resistive outer conductor of finite thickness. In Sec. VI the results are used to design an operational amplifier circuit that emulates the time dependence of a lossy conductor and allows one to measure the time-dependent current. Finally, in Sec. VII a number of useful graphs and analytic approximations are given.

II. SOLUTION OF DIFFUSION EQUATION

In this section we consider five special but typical geometrical shapes and boundary conditions. The cases chosen have sufficient symmetry that the normal component of the magnetic field is zero as the field diffuses into the conductor.

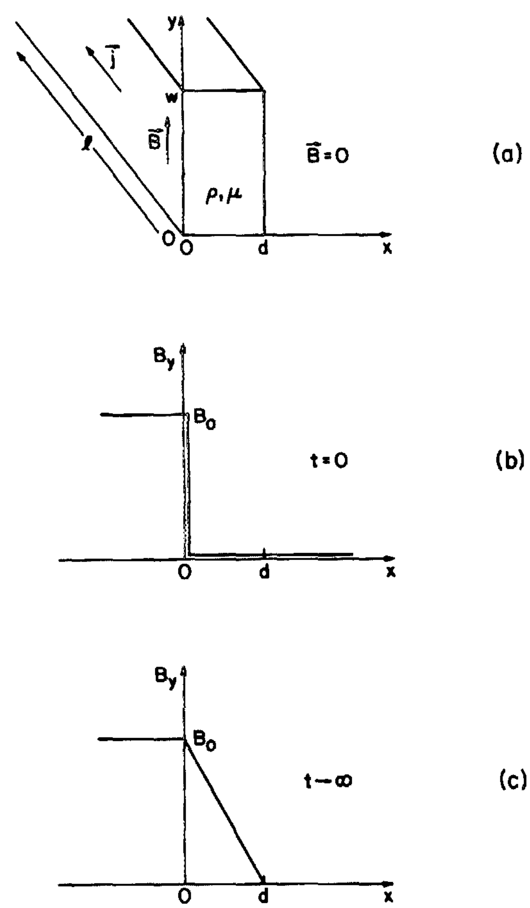

FIG. 1. Case A: Plane slab with uniform magnetic field on one face (a) with solution at $t = 0$ (b) and $t \to \infty$ (c).

 0021-8979/86/140475-07$02.40

A. Plane slab with magnetic field on one face

Consider first a plane slab of conductor of resistivity ρ, permeability μ, and thickness d with a current density $j_z(x,t)$ that produces a uniform magnetic field B_0 in the y direction on one face and no magnetic field on the other face, as shown in Fig. 1. The diffusion equation for magnetic field in the slab is

$$\frac{\partial B_y}{\partial t} = \frac{\rho}{\mu}\frac{\partial^2 B_y}{\partial x^2}. \tag{1}$$

The general solution inside the slab is a superposition of a constant term, a term proportional to x with no t dependence, and a term that can be written as a product of some function of space and some function time. The first two terms can be determined from the boundary conditions as $t\to\infty$. The third term is then found by the method of separation of variables and Fourier analysis to match the initial condition at $t=0$. The result is given by

$$B_y(x,t) = B_0\left(1 - \frac{x}{d} - 2\sum_{n=1}^{\infty}\frac{\sin(n\pi x/d)}{n\pi}e^{-\pi^2 n^2 \rho t/\mu d^2}\right). \tag{2}$$

B. Plane slab with the same magnetic field on each face

Consider now a plane slab of thickness d as above but with a uniform magnetic field B_0 in the same direction on each face as shown in Fig. 2. The diffusion equation is the same as Eq. (1). The solution for the magnetic field in the slab as a function of time is derived as above and is given by

$$B_y(x,t) = B_0\left(1 - 4\sum_{\substack{n=1\\ n\ \text{odd}}}^{\infty}\frac{\sin(n\pi x/d)}{n\pi}e^{-\pi^2 n^2 \rho t/\mu d^2}\right). \tag{3}$$

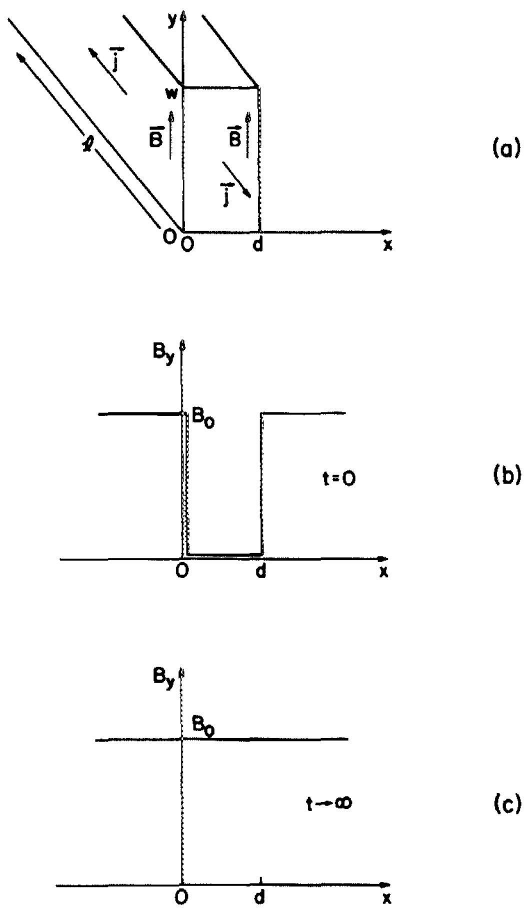

FIG. 2. Case B: Plane slab with uniform magnetic field in the same direction on each face (a) with solution at $t=0$ (b) and $t\to\infty$ (c).

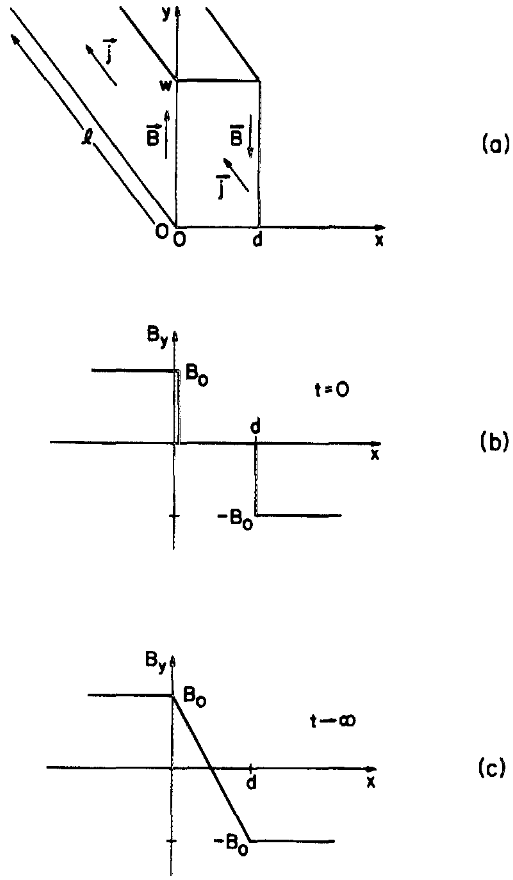

FIG. 3. Case C: Plane slab with uniform magnetic field in opposite directions on the two faces (a) with solution at $t=0$ (b) and $t\to\infty$ (c).

C. Plane slab with opposite magnetic field on the two faces

Consider now a plane slab of thickness d as above but with a uniform magnetic field B_0 of opposite sign on each face as shown in Fig. 3. The diffusion equation is the same as Eq. (1). The solution for the magnetic field in the slab as a function of time is derived as above and is given by

$$B_y(x,t) = B_0\left(1 - \frac{2x}{d} - 4\sum_{\substack{n=2\\ n\ \text{even}}}^{\infty}\frac{\sin(n\pi x/d)}{n\pi}e^{-\pi^2 n^2 \rho t/\mu d^2}\right). \tag{4}$$

D. Cylindrical rod with axial current

Consider now a cylindrical conducting rod of resistivity ρ, permeability μ, and radius a with an axial current density $j_z(r,t)$ that produces a uniform azimuthal magnetic field B_0 in the θ direction at the surface of the rod as shown in Fig. 4.

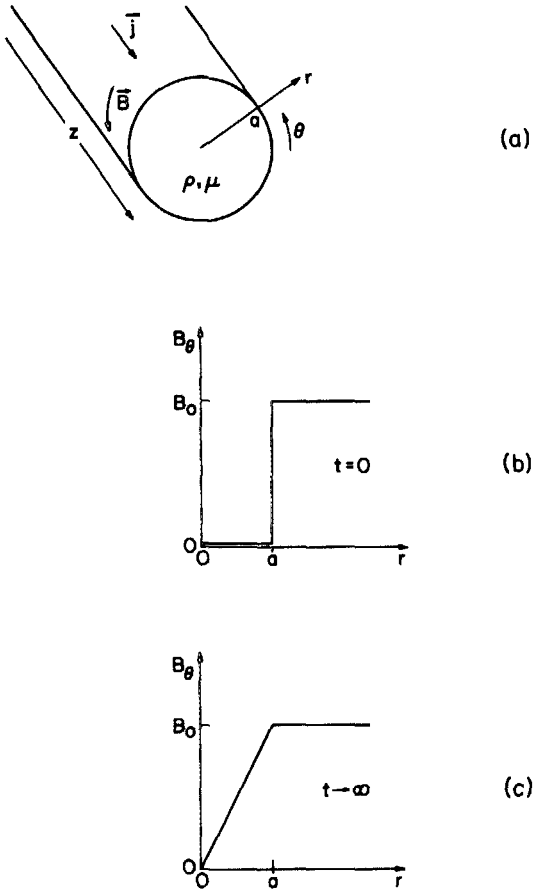

FIG. 4. Case D: Cylindrical rod with axial current (a) with solution at $t = 0$ (b) and $t \to \infty$ (c).

As before, the diffusion equation can be derived and has the form

$$\frac{\partial B_\theta}{\partial t} = \frac{\rho}{\mu}\left(\frac{\partial^2 B_\theta}{\partial r^2} + \frac{1}{r}\frac{\partial B_\theta}{\partial r} - \frac{B_\theta}{r^2}\right). \tag{5}$$

The general solution inside the rod is given by

$$B_\theta(r,t) = B_0\left(\frac{r}{a} + 2\sum_{n=1}^{\infty}\frac{J_1(p_n r/a)}{p_n J_0(p_n)}e^{-p_n^2\rho t/\mu a^2}\right), \tag{6}$$

where the p_n are the roots of the Bessel function $J_1(p_n) = 0$ and are given to within 0.06% for all n by $p_n \approx \pi(n + 0.25 - 0.03106/n)$.

E. Cylindrical rod with azimuthal current

Finally, consider a cylindrical conducting rod of resistivity ρ, permeability μ, and radius a with an azimuthal current density $j_\theta(r,t)$ associated with a uniform axial magnetic field B_0 in the z direction at the surface of the rod as shown in Fig. 5. As before, the diffusion equation can be derived and has the form

$$\frac{\partial B_z}{\partial t} = \frac{\rho}{\mu}\left(\frac{\partial^2 B_z}{\partial r^2} + \frac{1}{r}\frac{\partial B_z}{\partial r}\right). \tag{7}$$

The general solution inside the rod is given by

$$B_z(r,t) = B_0\left(1 - 2\sum_{n=1}^{\infty}\frac{J_0(q_n r/a)}{q_n J_1(q_n)}e^{-q_n^2\rho t/\mu a^2}\right), \tag{8}$$

where the q_n are the roots of the Bessel function $J_0(q_n) = 0$ and are given to within 0.03% for all n for $q_n \approx \pi(n - 0.25 + 0.01525/n)$.

III. TIME-DEPENDENT IMPEDANCE FOR STEP FUNCTION CURRENT

If the current I that produces the magnetic field B_0 at the surface of the conductor turns on abruptly at $t = 0$, the time-dependent impedance can be calculated from

$$Z(t) = \frac{V(t)}{I} = \frac{\int \mathbf{E}_0(t)\cdot d\mathbf{l}}{I} = \frac{\int \rho \mathbf{j}_0(t)\cdot d\mathbf{l}}{I}, \tag{9}$$

where $V(t)$ is the voltage drop along some length at the surface of the conductor and $\mathbf{j}_0(t)$ is the current density at the surface.

For the plane slab with field on one face (case A of Sec. II), the current density is $j_z = \partial B_y/\partial x/\mu$, and the total current is $I = -B_0 w/\mu$, where w is the width of the slab, and d is assumed much smaller than w. Differentiating Eq. (2) and substituting into Eq. (9), integrating E all the way around the slab ($2w$), gives

$$Z(t) = \frac{\rho l}{wd}\left(1 + 2\sum_{n=1}^{\infty} e^{-\pi^2 n^2 \rho t/\mu d^2}\right), \tag{10}$$

where l is the length of the slab.

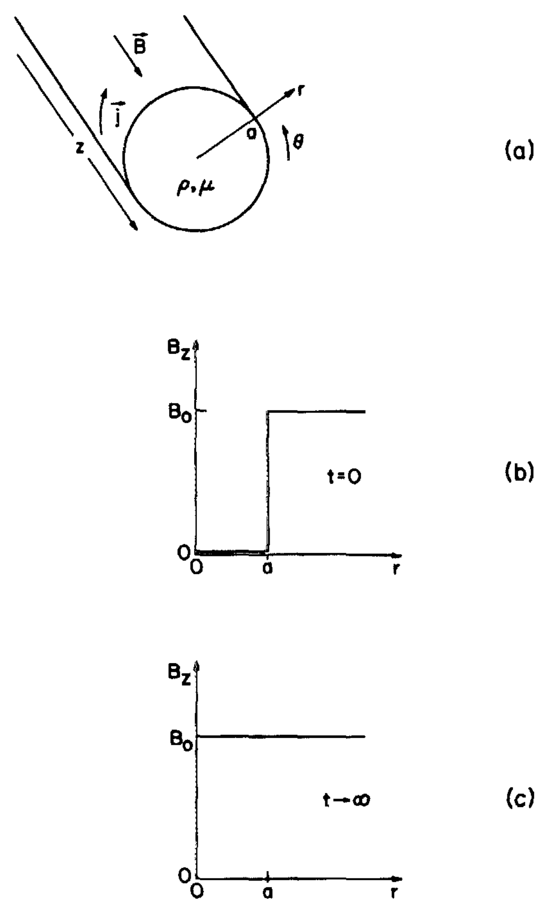

FIG. 5. Case E: Cylindrical rod with azimuthal current (a) with solution at $t = 0$ (b) and $t \to \infty$ (c).

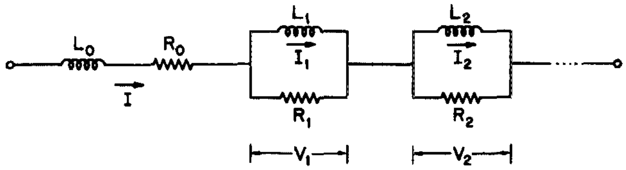

FIG. 6. Electrical equivalent circuit representation for the time-dependent impedances calculated in Sec. III. See Table I for values of components.

For the plane slab with the same field on both faces (case B of Sec. II), the procedure is the same except that the current density at the surface is determined by differentiating Eq. (3) to get the result:

$$Z(t)=\frac{8\rho l}{wd}\sum_{n=1}^{\infty}e^{-\pi^2(2n-1)^2\rho t/\mu d^2}. \tag{11}$$

Note that the current used in Eq. (9) is the constant, external current that produces the field B_0 at the conductor and not the induced current in the conductor that decays away in time. This definition of impedance is necessary for the electrical circuit model to be described in the next section.

For the plane slab with opposite fields on each face (case C of Sec. II), the procedure is the same except that the current density at the surface is determined by differentiating Eq. (4) to get the result:

$$Z(t)=\frac{\rho l}{wd}\left(1+2\sum_{n=1}^{\infty}e^{-4\pi^2n^2\rho t/\mu d^2}\right). \tag{12}$$

For the cylindrical rod with axial current (case D of Sec. II), the current density is $j_z=(\partial B_\theta/\partial r+B_\theta/r)/\mu$, and the total current is $I=B_0 2\pi a/\mu$. Differentiating Eq. (6) and substituting into Eq. (9) gives

$$Z(t)=\frac{\rho l}{\pi a^2}\left(1+\sum_{n=1}^{\infty}e^{-p_n^2\rho t/\mu a^2}\right), \tag{13}$$

where l is the length of the cylinder.

Finally, for the cylindrical rod with azimuthal current (case E of Sec. II), the current density is $j_z=\partial B_z/\partial r/\mu$, and the external driving current is $I=-B_0 l/\mu$, where l is the length of the rod. Differentiating Eq. (7) and substituting into Eq. (9) with the electric field integrated once around the circumference $2\pi a$ gives

$$Z(t)=\frac{4\pi\rho}{l}\sum_{n=1}^{\infty}e^{-q_n^2\rho t/\mu a^2}. \tag{14}$$

IV. ELECTRICAL EQUIVALENT CIRCUITS

The time-dependent impedances derived in Sec. III have the limitation that they apply only for step function currents. On the other hand, any physical waveform can be decomposed into an infinite sum of step functions with varying amplitudes and starting times. Thus, if we can represent the impedance in terms of an electrical equivalent circuit in such a way that it responds correctly for an arbitrary step function, then it will have the correct response for any time-varying current, and the skin effect can be analyzed by ordinary circuit analysis techniques.

A common characteristic of all the solutions is an infinite sum of exponential terms with a time-dependent amplitude and progressively shorter time constants. The amplitude of each term in $Z(t)$ happens to be the same on the surface of the conductor where the voltage is measured. This suggests a linear electrical equivalent circuit representation as shown in Fig. 6. In this representation, L_0 is the inductance of the space external to the conductor and is calculated by conventional means as if the conductor had zero resistivity and completely excluded the magnetic field from its interior. R_0 is the dc resistance that the conductor has after the field has soaked completely through. The RL networks are arranged so that the R_n values are all equal to R_1 and the time constants $\tau_n=L_n/R_n$ match the time constants $\exp(-t/\tau_n)$ of each term in the series. The values required for each of the five cases considered in Sec. II are given in Table I.

To use the circuit representation, one would typically truncate the series after some finite number of terms. This is equivalent to neglecting the very fast transient behavior of the circuit (times shorter than $\tau_{n\,\max}$). When this is done, it is sometimes important to add whatever inductance has been ignored to L_0. For this purpose, the sum of the inductances from $n=1$ to ∞ is included in Table I. This sum is a useful

TABLE I. Parameters for the circuit in Fig. 6 and the analytical representations in Sec. VII. [Note: $p_n\approx\pi\,(n+0.25-0.03106/n)$, $q_n\approx\pi\,(n-0.25+0.01525/n)$.]

Case	A	B	C	D	E
R_0	$\rho l/wd$	0	$\rho l/wd$	$\rho l/\pi a^2$	0
R_1	$2R_0$	$8\rho l/wd$	$2R_0$	R_0	$4\pi\rho/l$
L_1	$2\mu ld/\pi^2 w$	$8\mu ld/\pi^2 w$	$\mu ld/2\pi^2 w$	$\mu l/\pi p_1^2$	$4\pi\mu a^2/q_1^2 l$
R_n	R_1	R_1	R_1	R_1	R_1
L_n	L_1/n^2	$L_1/(2n-1)^2$	L_1/n^2	$p_1^2L_1/p_n^2$	$q_1^2L_1/q_n^2$
ΣL_n	$\mu ld/3w$	$\mu ld/w$	$\mu ld/12w$	$\mu l/8\pi$	$\pi\mu a^2/l$
τ_1	$\mu d^2/\pi^2\rho$	$\mu d^2/\pi^2\rho$	$\mu d^2/4\pi^2\rho$	$\mu a^2/p_1^2\rho$	$\mu a^2/q_1^2\rho$
τ_n	τ_1/n^2	$\tau_1/(2n-1)^2$	τ_1/n^2	$p_1^2\tau_1/p_n^2$	$q_1^2\tau_1/q_n^2$
A	$\pi/4$	$\pi/16$	$\pi/4$	$p_1^2/4\pi$	$q_1^2/4\pi$
K	$3\sqrt{10}/\pi^2$	$4\sqrt{6}/\pi^2$	$3\sqrt{10}/\pi^2$	$8\sqrt{3}/p_1^2$	$4\sqrt{2}/q_1^2$
k	0.86	2.4	0.86	0.76	1.1
M	$6/\pi^2$	$8/\pi^2$	$6/\pi^2$	$8/p_1^2$	$4/q_1^2$
v/Z	$w/\mu l$	$w/\mu l$	$2w/\mu l$	$2\pi a/\mu l$	$1/\mu$

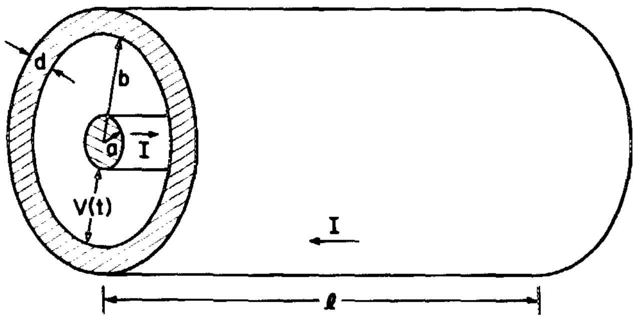

FIG. 7. Coaxial line with solid center conductor and thick outer conductor, shorted at one end and open at the other.

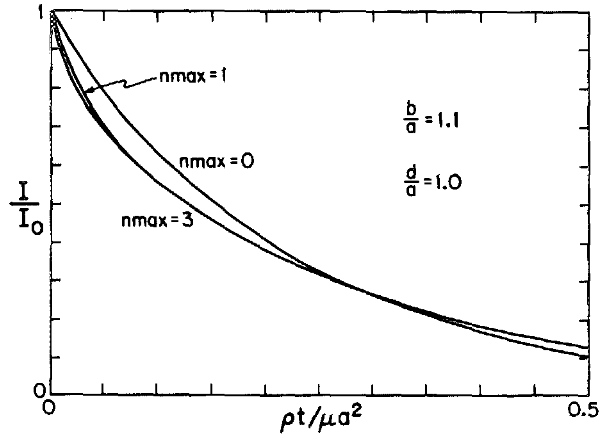

FIG. 9. Decay of current in the coaxial line in Fig. 7 as represented by the circuit in Fig. 8 including various number of terms of the infinite series.

quantity also because it is the internal inductance of the conductor after the field has soaked completely through.

Geometrical shapes more complicated than those considered above can often be treated as a superposition of the cases considered by placing the various circuits in series with one another. Then one must be careful not to doubly count the inductance L_0.

V. EXAMPLE: COAXIAL LINE

As an example of the methods outlined above, consider a coaxial line of length l, with a free space of inner radius a, and outer radius b as shown in Fig. 7. The center conductor and the outer conductor are solid with resistivity ρ and permeability μ. The outer conductor has thickness d. The line is long compared with its radius, but not so long that transmission line effects (distributed capacitance) are important (i.e., the line is short compared with the free space wavelength). The line is shorted at one end, and we wish to model the impedance as seen from the other end by an electrical equivalent circuit.

Following the procedure in Sec. IV, we represent the line as shown in Fig. 8. Here we have kept only the first three terms representing field diffusion into the center conductor (case D) and the first three terms for diffusion into the outer conductor which we treat in the plane slab approximation using a width $2\pi b$ (case A). The inductance of the space between the conductors is the familiar $\mu_0 \ln(b/a)/2\pi$, but

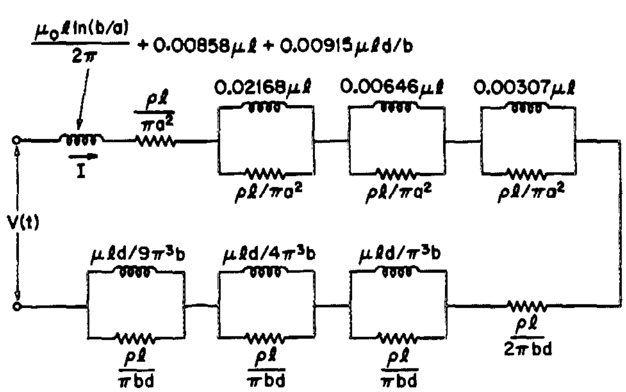

FIG. 8. Electrical equivalent circuit representation for the coaxial line in Fig. 7 including three terms of each infinite series.

with a correction added to account for the sum of the inductances interior to the conductors for $n > 3$. The impedance of the short at the end has been neglected. Recognize the dc resistance of the inner conductor ($\rho l/\pi a^2$) and the outer conductor ($\rho l/2\pi bd$). The values have been taken from Table I.

As a specific numerical example, suppose we take $\mu = \mu_0$, $b/a = 1.1$, and $d/a = 1$ and measure time in the natural units of $\mu a^2/\rho$. We take $V(t) = 0$ and an initial condition of $I(t = 0) = I_0$ and solve the circuit equations numerically as the current decays. This corresponds to a voltage step function down from some initial, constant value ($I_0 R_0$) to zero. The length of the line l does not matter since all resistances and inductances are proportional to l. The results are shown in Fig. 9 for $n$max $= 0$ (no time-dependent soak-in), $n$max $= 1$, and $n$max $= 3$ (the case in Fig. 8). For this case the skin effect is not very dramatic and is very accurately modeled with as few as three terms in the infinite series. Soak-in is a much less prominant effect for a step function voltage than for a step function current. It is most important for situations in which the external inductance is small ($L_0 \ll L_1$).

VI. OPERATIONAL AMPLIFIER EMULATION

In many instances it is desirable to have a means to measure an electrical current that is partially soaked into a conductor and to convert the measurement into a time-dependent voltage for observation or recording. The usual methods consist of either measuring the voltage drop along the surface of the conductor and dividing by the resistance or integrating the voltage signal from a loop that encloses some portion of the magnetic flux produced by the current and dividing by the inductance. For the cases considered here, neither the resistance nor inductance are constant, and a different approach is required. The desired operation is exactly the one performed by the electrical circuit in Fig. 6. Thus, if we were to construct the circuit in Fig. 6 and connect it across the terminals of the conductor, the current could be determined by reading the voltage across resistor R_0 for any waveform.

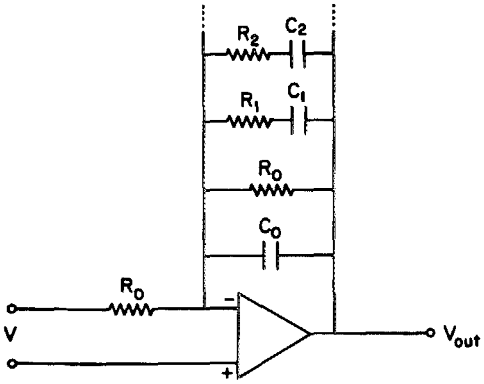

FIG. 10. Operational amplifier circuit that permits measurement of the current in a conductor in which the magnetic field is partially soaked in.

In practice, it is usually more convenient to construct circuits with capacitors rather than inductors, and such a circuit using an operational amplifier is shown in Fig. 10. The resistance values are the same as in Table I, and the capacitors are chosen so that the time constant of each RC branch matches the time constant of the corresponding RL branch in Fig. 6 (i.e., $C_n = L_n/R_n^2$ for $n = 0$ to ∞). The resistors and capacitors in Fig. 10 could be changed to give any convenient output voltage from the amplifier ($V_{\rm out} = -IR_0^2/R_{\rm in}$), so long as all the time constants ($R_n C_n$) are preserved. The circuit in Fig. 10 can be thought of as the usual active integrator that determines the current from $V = LdI/dt$ but with additional components in the feedback loop to account for the time-dependent resistance and internal inductance of the conductor.

VII. GRAPHICAL AND ANALYTICAL REPRESENTATION OF RESULTS

For all the cases considered in Sec. II, the time-dependent impedance derived in Sec. III for a step function of current has the form

$$Z(t) = R_0 + R_1 \sum_{n=1}^{\infty} e^{-t/\tau_n}, \tag{15}$$

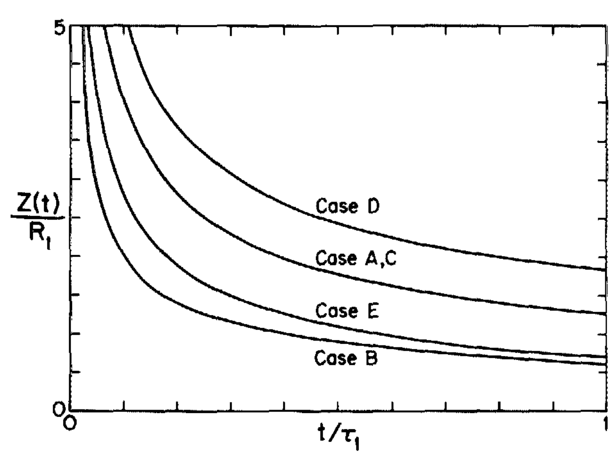

FIG. 11. Impedance as a function of time for a step function of current for each of the five cases described in Sec. II.

where R_0 may be zero (cases B and E) and the parameters are defined in Table I. Graphs of the impedance versus time for the five cases are shown in Fig. 11. Note that skin effect is very dramatic for current steps, in contrast to the small effect for voltage steps shown in Sec. V.

For many purposes it is useful to have an analytical approximation to Eq. (15) that does not involve an infinite series. In the limit of $t \to \infty$, the first ($n = 1$) term in the sum dominates, and the impedance decays asymptotically to R_0 in a simple exponential fashion with time constant τ_1.

In the limit of $t \to 0$, the current flows in a thin skin on the surface, and the diffusion equation is the same for all cases and can be solved to give an impedance of the form

$$Z(t) \to (l/w)\sqrt{\mu\rho/\pi t} \text{ for } t \to 0, \tag{16}$$

where l is the length in the direction of the current and w is the distance along the surface of the conductor in the direction of the magnetic field (as in case A).

A function with the correct asymptotic limits is given by

$$Z(t) \approx R_0 + R_1[(A\tau_1/t)^3 + 1]^{1/6} e^{-t/\tau_1}, \tag{17}$$

where the constants A for the various cases are given in Table I. In Eq. (17) the exponents 3 and 1/6 have been chosen to produce a fit for all cases with a maximum error of approximately 10%. The worst error typically occurs at a time $t \approx 0.1\,\tau_1$ and varies from about 4% (for case E) to 11% (for case D). The fit overestimates the resistance for all cases except case B. The $t \to 0$ limit provides a check on the calculations that led to the values in Table I.

The electrical circuit in Fig. 6 also suggests a frequency-domain representation in terms of a complex impedance $Z(\omega)$ which is calculated to be

$$Z(\omega) = j\omega L_0 + R_0 + R_1 \sum_{n=1}^{\infty} \frac{\omega^2 L_n^2 + j\omega L_n R_1}{R_1^2 + \omega^2 L_n^2}. \tag{18}$$

If we equate this impedance to $R(\omega) + j\omega L(\omega)$, the frequency-dependent resistance becomes

$$R(\omega) = R_0 + R_1 \sum_{n=1}^{\infty} \frac{\omega^2 \tau_n^2}{1 + \omega^2 \tau_n^2} \tag{19}$$

and the frequency-dependent inductance becomes

$$L(\omega) = L_0 + \sum_{n=1}^{\infty} \frac{L_n}{1 + \omega^2 \tau_n^2}, \tag{20}$$

where the parameters are given in Table I.

Graphs of the resistance and inductance versus frequency for the five cases are shown in Figs. 12 and 13. The inductance in Fig. 13 is just the portion internal to the conductor and thus asymtotically approaches zero for all cases as $\omega \to \infty$, since the magnetic field is excluded from the conductor in that limit.

As was the case for the step function current, it is useful to have analytical approximations to Eqs. (19) and (20) that do not involve infinite series. In the limit of $\omega \to 0$, the denominator of Eqs. (19) and (20) become unity, and the result is a simple summation:

$$R(\omega) \to R_0 + R_1(\omega\tau_1)^2 \sum_{n=1}^{\infty} \left(\frac{\tau_n}{\tau_1}\right)^2 \quad \text{for } \omega\tau_1 \ll 1, \tag{21}$$

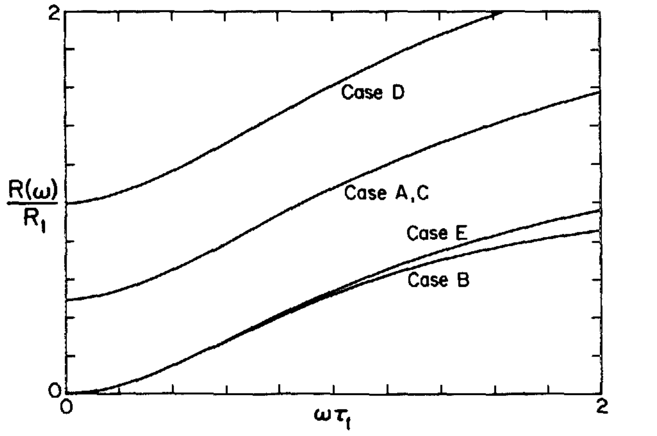

FIG. 12. Resistance as a function of the sinusoidal frequency for each of the five cases described in Sec. II.

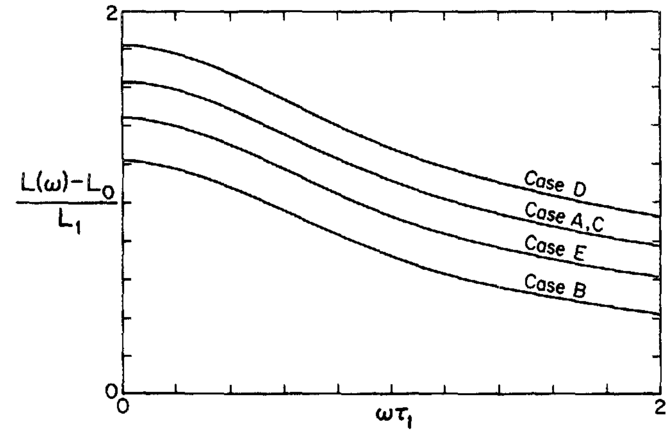

FIG. 13. Internal inductance as a function of the sinusoidal frequency for each of the five cases described in Sec. II.

$$L(\omega)\rightarrow L_0+\sum_{n=l}^{\infty} L_n \quad \text{for } \omega\tau_1 \ll 1. \tag{22}$$

The summation in Eq. (21) is a constant K^2. The quantity K and the summation of L_n in Eq. (22) are given in Table I.

In the limit of $\omega\rightarrow\infty$, the current flows in a thin skin on the surface, and the resistance can be calculated as if the current density were uniform over a distance equal to the skin depth given by

$$\delta=\sqrt{2\rho/\mu\omega}. \tag{23}$$

Thus, for all cases the resistance has the form

$$R(\omega)\rightarrow \rho l/w\delta \quad \omega\tau_1 \gg 1, \tag{24}$$

where l is the length in the direction of the current and w is the distance along the surface of the conductor in the direction of the magnetic field (as in case A). Similarly, the inductance in the limit of $\omega\rightarrow\infty$ is given by

$$L(\omega)\rightarrow L_0+(\mu l\delta/2w) \quad \text{for } \omega\tau_1 \gg 1. \tag{25}$$

Note that in this limit the internal reactance $\omega[L(\omega)-L_0]$ and the resistance $R(\omega)$ are equal, and thus the phase between the voltage measured at the surface of the conductor and the total current in the conductor is 45°. At small ω the impedance is resistive when $R_0>0$ (cases A, C, and D) and reactive when $R_0=0$ (cases B and E).

Functions with the correct asymptotic limits are given by

$$R(\omega)\approx R_0+R_1[(K/\omega\tau_1)^{2k}+(2/\pi A\omega\tau_1)^{k/2}]^{-1/k} \tag{26}$$

and

$$L(\omega)\approx L_0+L_1[M^6+(2\omega\tau_1/\pi A)^3]^{-1/6}, \tag{27}$$

where the constants are given in Table I. The exponent k has been chosen to produce a fit for all cases with a maximum error of approximately 10% except for the inductance for case B for which the maximum error is about 27%.

Finally, we remark that for some purposes it is useful to know the speed with which magnetic field lines diffuse into the surface of a conductor. This number determines, for example, how effective a conductor is as a magnetic shield. Since the diffusion speed is given by $v=E/B$ and since E is proportional to the voltage and B is proportional to the current, the speed at the surface has the same time-dependence as the impedance and a proportionality factor that depends upon the geometry as given in the last entry in Table I.

VIII. SUMMARY

In this paper the time-dependent diffusion equation has been solved for five, special, but typical, geometrical shapes. The solution permits the definition of a time-dependent impedance for the special case of a step function current. The impedance can be written as an infinite sum of exponentials with constant amplitude and progressively shorter time constants. The impedance suggests a linear electrical equivalent circuit representation that is valid for any time-dependent waveform and allows solution by conventional circuit analysis techniques. As an example, the technique is used to calculate the current response to a step function voltage for a coaxial line. The electrical properties of conductors with skin effect can be emulated by an operational amplifier with a number of RC branches in its feedback loop. Such a circuit provides a practical method of determining the time-dependent current in a conductor by measuring some appropriate external voltage. Finally, graphical and analytical representations of the results are given for the case of a step function current and for a sinusoidal current.

ACKNOWLEDGMENTS

This work was supported by the U. S. Department of Energy and the National Science Foundation.

[1] H. B. Dwight, Trans. Am. Inst. Electr. Eng. **37**, 1379 (1918).
[2] W. H. Bostick, in *Pulse Generators*, Massachusetts Institute of Technology Radiation Laboratory Series (McGraw-Hill, New York, 1948), p. 617.
[3] H. G. B. Casimir and J. Ubbink, Phillips Tech. Rev. **28**, 271 (1967).
[4] V. F. Aleksin and S. S. Romanov, Sov. Phys. Tech. Phys. **18**, 724 (1973).
[5] J. Weiss and V. K. Garg, IEEE Trans. Magn. **MAG-21**, 2313 (1985).
[6] A. Konrad, M. V. K. Chari, and Z. J. Csendes, IEEE Trans. Magn. **MAG-18**, 450 (1982).
[7] C. S. Biddlecomb, E. A. Heighway, J. Simkin, and C. W. Trowbridge, IEEE Trans. Magn. **MAG-18**, 492 (1982).
[8] J. R. Brauer, IEEE Trans. Magn. **MAG-18**, 504 (1982).